bioresources.com

Transformation and Products Distribution of Moso Bamboo and Derived Components During Pyrolysis

Xue-Yong Ren,[a] Zhong-Tao Zhang,[a,b] Wen-Liang Wang,[a] Hui Si,[c] Xiao Wang,[c] and Jian-Min Chang [a,*]

Transformation and products distribution of moso bamboo (*Phyllostachys edulis*) and its derived components during pyrolysis were investigated by thermogravimetric analyzer coupled with Fourier transform infrared spectrometry (TG-FTIR) and analytical pyrolysis coupled with gas chromatography/mass spectrometry (Py-GC/MS) techniques. The pyrolysis of moso bamboo was generally an integrated result of the decomposition of its several derived components by examining the degradation process parameters and pyrolysis kinetics. The main peaks of the infrared (IR) spectrum for gases released at the highest intensity were assigned to be CO_2, CO, CH_4, H_2O, acids, aldehydes, aromatics, ethers, and alcohols. Pyrolysis temperature played an important role in the products distribution of moso bamboo by affecting the products' yield and secondary cracking of heavy compounds. 500 °C was an inflection point for product release during moso bamboo pyrolysis. Further cracking of aromatic compounds and furans into lighter products was observed with increasing pyrolysis temperature.

*Contact information: a: College of Materials Science and Technology, Beijing Forestry University, Beijing 100083, China; b: Planning & Design Institute of Forest Products Industry, State Forestry Administration, Beijing, 100010, China; c: College of Technology, Beijing Forestry University, Beijing 100083, China; *Corresponding author: cjianmin@bjfu.edu.cn*

INTRODUCTION

Due to the limited reserves of fossil resources and the environmental burden during their utilization processes, more and more interest is being put on the application of biomass, which is considered to be a renewable and green resource. Bamboo is a kind of fast-growing biomass, which has great potential as a bio-energy resource of the future. Moso bamboo is the most abundant kind of bamboo in China, widely cultivated in the west and south of China, with an annual yield of about eighteen million tons (Jiang *et al*. 2012).

An important biomass, moso bamboo can be converted into biofuels by thermal chemical methods, mainly including pyrolysis, gasification, and liquefaction. The products of the thermo–chemical conversion process can be typically divided into bio-oil, char, and gases. Bio-oil can be upgraded into bio-fuels or used to make value-added chemicals, while char is a good feedstock of activated carbon or soil amendment, and gases can be burned for energy recovery or used to produce syngas (Bridgwater 2012; Czernik and Bridgwater 2004; Laird *et al*. 2009; Lu *et al*. 2009).

In addition to the fast pyrolysis process for bio-oil production, the gasification and liquefaction processes usually couple with the pyrolysis reaction of feedstock. Pyrolysis reaction is the basis and foundation of many thermo–chemical processes. Therefore, to research and understand the pyrolysis properties and conversion process of moso

bamboo, it would be very helpful to better design the thermo–chemical process used for making bamboo into valuable biofuels and chemicals.

There has been some research on pyrolysis of various kinds of biomass materials. Cellulose is one of the well-studied bio-materials for pyrolysis, with many results of its thermal decomposition properties and conversion pathways (Hajallgol *et al*. 1982; Lédé 2012; Li *et al*. 2001; Lin *et al*. 2009; Mamleev *et al*. 2007; Ronsse *et al*. 2012). Hemicelluloses extracted and purified from switchgrass were studied for primary pyrolysis product distribution, and a total of 16 products were identified and quantified (Patwardhan *et al*. 2011). Lignin extracted from prairie cordgrass, aspen, and kraft lignin were used as feedstock for pyrolysis, and the effects of variability of lignin sources on pyrolysis products were investigated by Py-GC/MS and TG-FTIR (Zhang *et al*. 2012). Pyrolysis characteristics of raw bamboo were also investigated by several researchers using TG-FTIR and a fluidized bed reactor (Jiang *et al*. 2012; Jung *et al*. 2008). Liu *et al.* studied the composition of evolved volatiles from fast pyrolysis of tobacco stem by Py-GC/MS analysis, and the evolution patterns of the major products were investigated by TG-FTIR and TG-MS (Liu *et al*. 2013).

Although these previous researchers made remarkable headway in understanding the thermal decomposition and pyrolysis properties of various kinds of biomass, the transformation process and products distribution of moso bamboo pyrolysis, especially its comparability with derived components, have not been fully investigated. Moreover, the products' characteristics of biomass pyrolysis play a decisive role in its viability to be used for bio-chemicals and bio-fuels (Liu *et al*. 2013). The purpose of this study was to investigate the transformation properties and products distribution of moso bamboo pyrolysis and correlation to its derived components by thermogravimetric Fourier transform infrared spectroscopy (TG-FTIR) and pyrolysis gas chromatography/mass spectrometry (Py-GC/MS). By comparing the pyrolysis properties of raw materials and their compositional members, more mechanisms can be revealed about how the individual components contribute to the resultant thermal–chemical conversion behavior of moso bamboo.

EXPERIMENTAL

Materials

Moso bamboo (*Phyllostachys edulis*), collected from Shaowu City, Fujian Province, China, was used as the raw material in this study. The materials were air-dried and screened into a particle size of 40–60 mesh. Cellulose, holo-cellulose, and Klason lignin were prepared and collected during the composition analysis procedures (see the *Composition analysis* section). The derived components extracted from moso bamboo were dried under vacuum for several days and then stored in sealed vials.

Methods
Ultimate and proximate analysis

Carbon, hydrogen, and nitrogen contents of moso bamboo were measured according to Chinese National Standard GB/T 19143-2003 using a Vario EL III Elemental Analyzer. Oxygen content was calculated by difference. The proximate analysis was performed with a muffle furnace according to Chinese National Standard GB/T 212-2008. The results of ultimate and proximate analysis are shown in Table 1.

bioresources.com

Table 1. Ultimate Analysis and Proximate Analysis of Moso Bamboo

Elements	Ultimate Analysis				Proximate Analysis			
	C_{ad}	H_{ad}	O_{ad}	N_{ad}	$Moisture_{ad}$	$Volatiles_{ad}$	Fixed $Carbon_{ad}$	Ash_{ad}
Value	50.21	5.63	42.93	1.23	9.28	75.04	14.56	1.12
$_{ad}$, air-dried basis; O_{ad}, obtained by difference.								

Composition analysis

Composition analysis was performed according to Chinese National Standards for fibrous raw materials. Generally, 2 g of moso bamboo samples were extracted for 6 h in a Soxhlet apparatus by benzene–alcohol (2:1, v/v) or hot water. Then, the extractive-free materials were treated by nitric acid–alcohol (1:4, v/v) solution for the cellulose test, 0.5 mL glacial acetic acid and 0.6 g sodium chlorite for holo-cellulose, and 72% sulfuric acid solution and 3% sulfuric acid solution in sequence for the Klason lignin test. The composition of moso bamboo is summarized in Table 2.

Table 2. Composition Analysis of Moso Bamboo

Content	Cellulose (%)	Holo-cellulose (%)	Klason lignin (%)	Extractives (%)	
				Benzene–alcohol	Hot water
Value	42.87	71.36	24.26	4.79	6.31

TG-FTIR analysis

The TG-FTIR instrument used in this study consisted of a NETZSCH STA449F3 thermogravimetric analyzer (TG) coupled with a Bruker TENSOR 27 FTIR spectrometer. Approximately 5 mg of samples were used in each test. The experiment was carried out on a thermo balance at a linear heating rate of 20 °C • min^{-1} within the temperature range from the ambient to 850 °C. Nitrogen with a flow rate of 50 mL • min^{-1} was used for the carrier gas in order to provide an inert atmosphere. The spectrum scope of FTIR was in the range of 500 to 4000 cm^{-1} and the resolution factor was selected to be 1 cm^{-1}.

Computation method for the TG kinetics

Data from TG and DTG curves for the pyrolysis of moso bamboo and derived components were used to determine the kinetic parameters. Basically, the pyrolysis process is assumed to be controlled primarily by chemical decomposition. Coats and Redfern performed the mathematical analysis by the integral method (Coats and Redfern 1964).

$$\ln\left[\frac{g(\alpha)}{T^2}\right] = \ln\left[\frac{AR}{\beta E}\left(1 - \frac{2RT}{E}\right)\right] - \frac{E}{RT} \tag{1}$$

The 3D-diffusion model was applied here for the expression form of g(α) as follows (Guo and Lua 2001),

$$g(\alpha) = \left[1 - (1 - \alpha)^{\frac{1}{3}}\right]^2 \tag{2}$$

where g(α) is a function that describes the way the reaction interface occurs throughout the sample. The parameter α is the fraction of materials decomposed at time *t*, *A* is the

frequency factor, E is the activation energy of the reaction, R is the universal gas constant, 8.314462 J• mol^{-1}•K^{-1}, T is the reaction temperature, and β is the heating rate.

By plotting the mass loss data from the TG curves, kinetics parameters will be obtained. Generally, a straight regression line with a slope of E/R can be obtained by plotting $\ln\left[\dfrac{g(\alpha)}{T^2}\right]$ versus $1/T$. After deriving the value of E, the arithmetic mean value of $\left(1-\dfrac{2RT}{E}\right)$ can be calculated with the initial and final reaction temperatures. Finally, the frequency factor (A) is obtained from the intercept of the line.

Py-GC/MS analysis

Py-GC/MS analysis was tested on a CDS Pyroprobe 5150 pyrolyser coupled directly to a Shimadzu GC/MS-QP2010 Plus. Samples, 0.5 mg, were used in each experiment. During the pyrolysis process, samples were heated to the pre-set temperature at a rate of 20 °C/ms and held for 10 s before being put into the GC/MS analytical system. The GC separation of pyrolysis vapors was performed with a 60 m × 0.25 mm × 0.25 μm DM-5 column. Helium was used as the carrier gas with a constant flow rate of 1 mL/min at a 1:80 split ratio. The GC inlet was 250 °C with a split ratio of 100:1. The oven temperature was programmed to start at 40 °C for 5 min and then raised to 280 °C at the heating rate of 5 °C /min. The mass spectrometer was operated in EI mode at 70 eV, and the mass spectra were obtained from m/z 20 to 400. Peaks identification was completed using the NIST mass spectrum library and also the literature data of previous studies (Azeez *et al*. 2010; Kim *et al*. 2011; Lu *et al*. 2012; Ohra-aho *et al*. 2005).

RESULTS AND DISCUSSION

Pyrolysis Kinetic Analysis of Moso Bamboo and Its Derived Components

TG and DTG curves for the pyrolysis characteristics of moso bamboo and its derived components are shown in Fig. 1. Distinct differences were found among the pyrolysis behaviors of these samples with different weight-loss rate and reaction range.
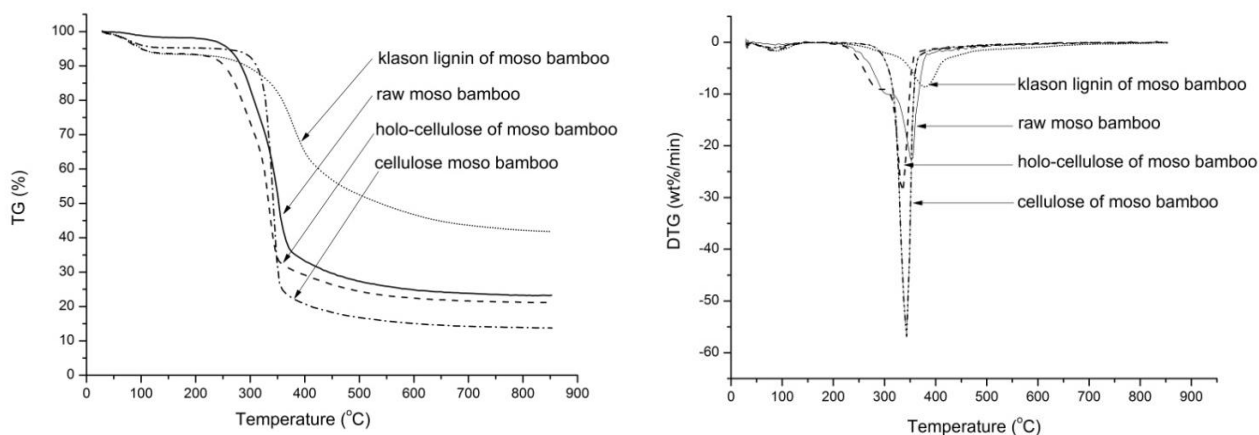

Fig. 1. TG and DTG curves of moso bamboo and its derived components during pyrolysis

Cellulose had the narrowest thermal decomposition temperature range and the lowest final residue content among all the samples, while lignin had the widest pyrolysis reaction range and the highest residue content. Cellulose pyrolysis was focused at a narrow temperature of 290 to 375 °C with the maximum weight loss rate (56.85 wt%/min) attained at 343 °C. The maximum pyrolysis reaction point of holo-cellulose was obtained at 336 °C with a DTG value of 21.13 wt%/min. Compared with cellulose, Klason lignin was the more difficult to decompose, with higher T_{max} value and slower and wider weight loss under the whole temperature range. Different from the orderly sacchariferous structure of cellulose, lignin is full of aromatic rings with various branches. The activity of the chemical bonds in lignin covered an extremely wide range, which led to the degradation of lignin occurring in a wide temperature range.

Table 3. Pyrolysis Kinetics Parameters of Moso Bamboo and Its Derived Components

Sample	Main Temp range/°C	T_{max}/ °C	DTG_{max}/ wt%/min	Residue/ wt%	Ea/ kJ • mol^{-1}	A/ min^{-1}	R^2
Raw moso bamboo	240-390	350	22.5	23.2	164.3	9.2×10^{12}	0.9934
Holo-cellulose from moso bamboo	220-400	336	28.8	21.1	123.9	6.2×10^{9}	0.9659
Cellulose from moso bamboo	290-375	343	56.9	13.8	317.5	1.7×10^{26}	0.9474
Klason lignin from moso bamboo	255-480	380	8.7	41.8	79.9	6.7×10^{5}	0.9657
*T_{max}, the temperature corresponding to the maximum DTG value DTG_{max}, the maximum value of derivative thermogravimetry in DTG curves E_a, apparent activation energy A, frequency factor R^2, correlation coefficient							

The pyrolysis kinetics parameters of moso bamboo were calculated by a 3-D diffusion model, shown in Table 3. Raw moso bamboo had an activation energy of 164.3 kJ • mol^{-1} and frequency factor of 9.2×10^{12} min^{-1}. The similar *Ea* value of moso bamboo by Coats-Redfern (modified) method was reported as around 150~200 kJ • mol^{-1} with corresponding conversion rate increasing from 10% to 70% (Jiang *et al.* 2012). As to the derived components, it was found that cellulose had the highest pyrolysis activation energy of 317.5 kJ • mol^{-1}, while Klason lignin had the lowest activation energy with only one fourth of that of cellulose. Cellulose is a semi-crystalline material, while lignin and hemicellulose are non-crystalline, so the decomposition of cellulose must first destroy the lattice structure of cellulose which needs extra energy, leading to its much higher activation energy than for hemicellulose and lignin. Mui *et al.* (2010) reported the similar cellulose pyrolystic kinetics parameters with activation energy of 326.8 kJ • mol^{-1} and frequency factor of 1.37×10^{22} min^{-1}. The residue content of the samples had the reverse rule to the activation energy, which means that as the sample decomposes more severely and with higher activation energy, its residue content becomes lower. It is worth notice that the pre-exponential factor of these several samples varied significantly. The frequency factor is a reflection of the frequency of collisions between reacting molecules (Jiang *et al.* 2010), so we can conclude that the pyrolysis of moso bamboo and its derived components had different reaction pathways.

The decomposition process parameters (reaction temperature ranges, T_{max}, DTG_{max}, and residue contents) and pyrolysis kinetics (E_a and A) of moso bamboo were numerically within the mutative scope of those characteristic parameters for its derived components. Therefore, the pyrolysis process of moso bamboo was generally an integrated result of the decomposing of its several derived components.

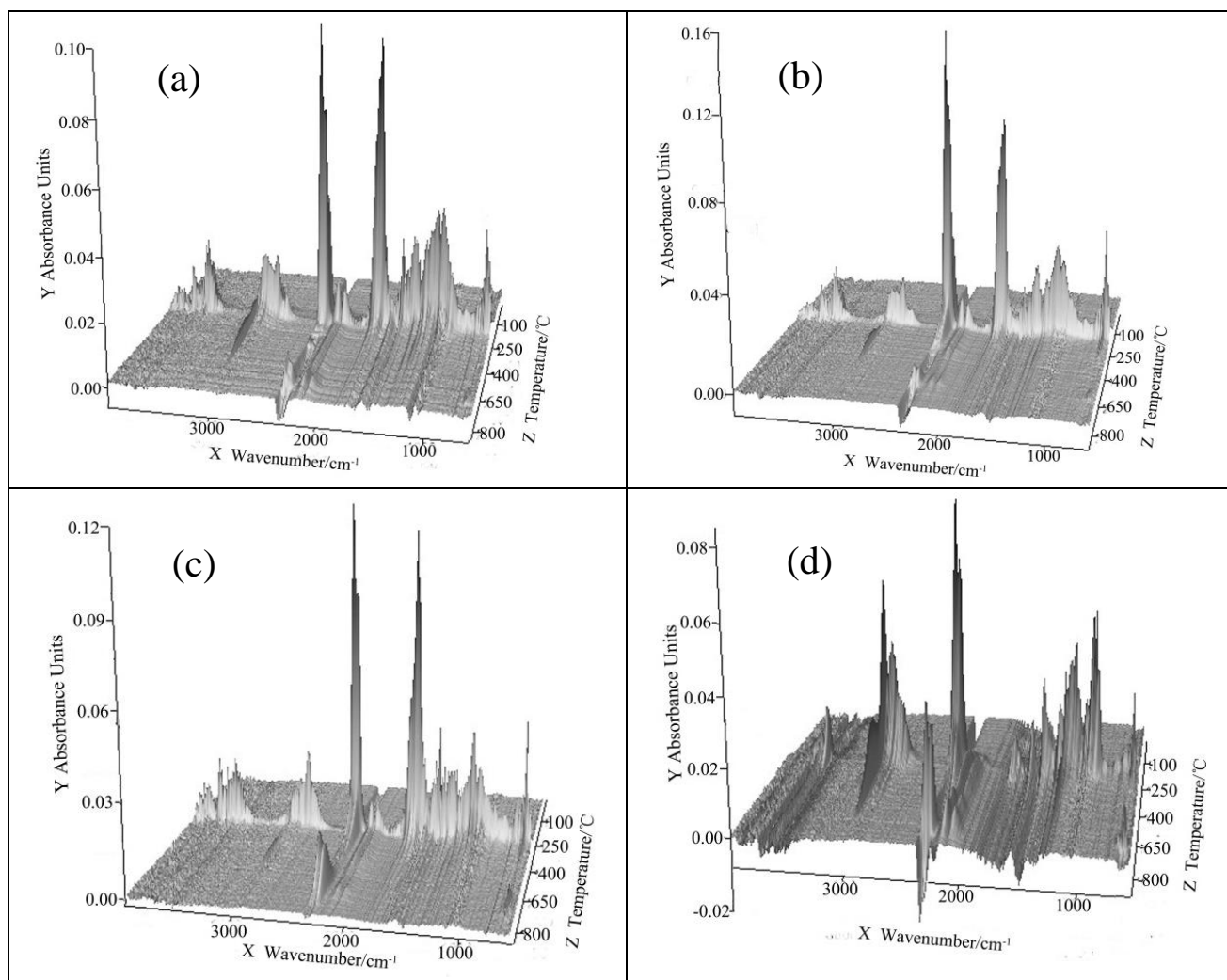## The Gaseous Products–Releasing Process of Moso Bamboo and Its Derived Components

Fig. 2. 3-D IR profiles of gas-product releasing from moso bamboo pyrolysis: (a) raw moso bamboo; (b) holo-cellulose from moso bamboo; (c) cellulose from moso bamboo; (d) Klason lignin from moso bamboo

The evolved volatiles from the TG pyrolysis of moso bamboo and its derived components were monitored by FTIR in real time (shown in Fig. 2). This indicates that the evolving profile of gas products during the pyrolysis process was a function of both wavenumber and temperature. Raw moso bamboo, cellulose, and holo-cellulose had similar patterns with a narrow evolving range and identical IR peaks, but with different releasing severity. Klason lignin was slightly different from other samples due to its

bioresources.com

specific pyrolysis properties with a wider evolving range of gas products. The release of gas products mainly happened at a temperature range of 300 to 400 °C, which corresponded well with the observation of weight-loss curves in Fig. 1. However, when the temperature reached 600 °C, there were still absorbance intensities of several peaks between 2400 and 2150 cm^{-1}. These were assigned to CO_2 and CO evolving out at a higher temperature, which was mainly ascribed to the further cracking and reforming of functional groups inside the volatiles at a later pyrolysis stage (Liu *et al*. 2013; Liu *et al*. 2008).
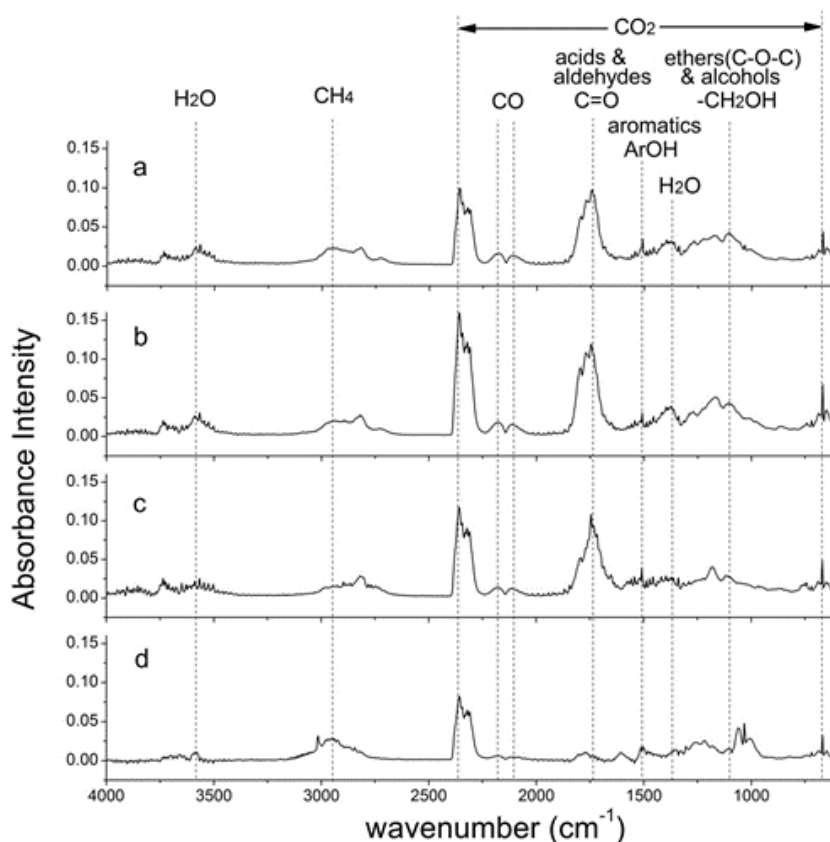

Fig. 3. IR spectra of gases released at the highest intensity value from moso bamboo and its derived components: (a) raw moso bamboo; (b) holo-cellulose from moso bamboo; (c) cellulose from moso bamboo; (d) Klason lignin from moso bamboo

Figure 3 shows the representative FTIR spectrums of several bamboo samples when the total released gas reached its highest intensity value. In earlier reports (Bassilakis *et al*. 2001; Guo *et al*. 2012; Liu *et al*. 2013; Liu *et al*. 2008; Yang *et al*. 2007), the main pyrolysis products of moso bamboo and its derived components were CO_2, CO, CH_4, H_2O, and some organics, such as acids, aldehydes, aromatics, ethers, and alcohols. The release of CO_2 was mainly caused by the cracking and reforming of functional groups of carboxyl (C=O) and COOH, or the reduction reaction of CO. Holo-cellulose gave the highest yield of carbon dioxide, which means that the release of CO_2 from biomass pyrolysis was mostly contributed by hemicellulose. As for the CO, it was mainly released from the cracking of carbonyl (C-O-C) and carboxyl (C=O). Cellulose and holo-cellulose had more release of carbon monoxide than lignin, which may be attributed to their different composition units. Methane was mainly formed by the cracking of

methoxyl-O-CH$_3$. Generally, bamboo lignin tended to produce more methane, possibly due to its higher methoxyl (-OCH$_3$) content. Water was produced from various kinds of dehydration reactions or polycondensation processes. The release of organic compounds mainly originated from the direct cracking and decomposition of the biomass samples. Acids and aldehydes were mainly created by the decomposition of saccharides from cellulose or hemicellulose, while lignin released few of them in its pyrolysis process.

Products Distribution of Moso Bamboo with Different Pyrolysis Temperature
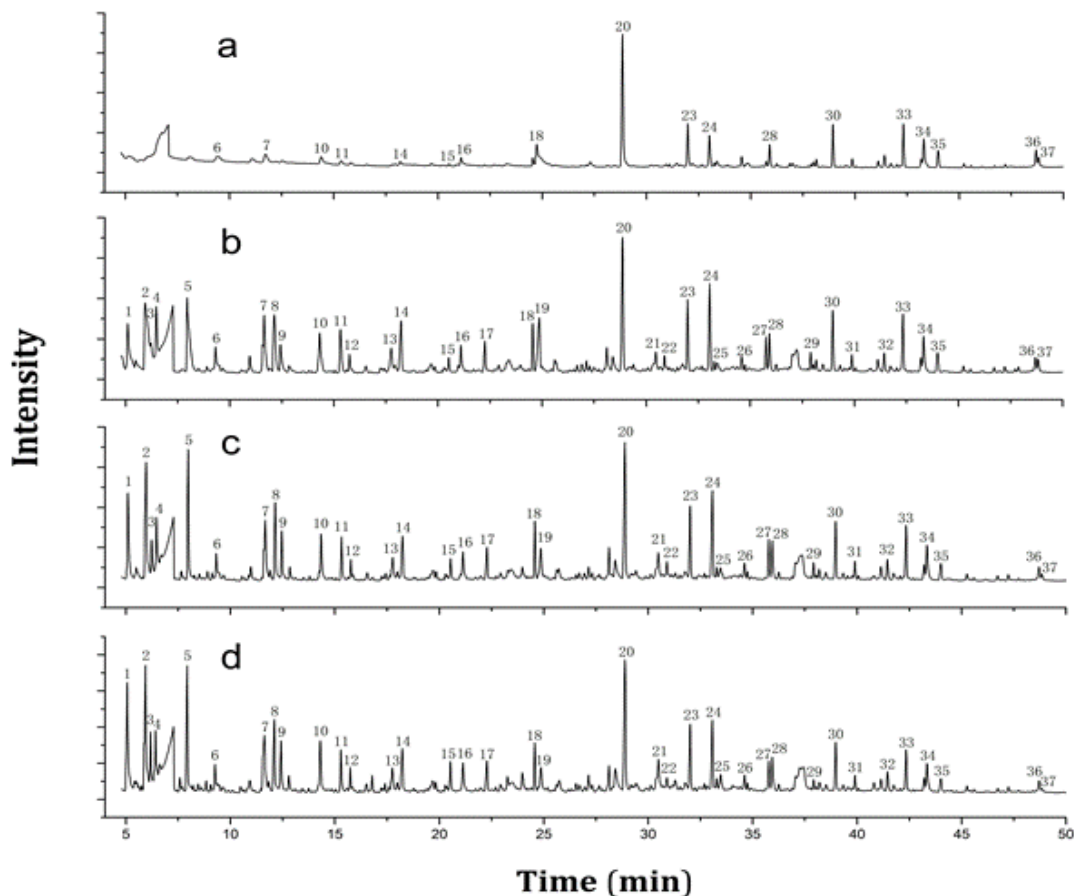

Fig. 4. Py-GC/MS of moso bamboo at different pyrolysis temperatures: (a) 400 °C; (b) 500 °C; (c) 600 °C; (d) 700 °C.

Fast pyrolysis temperature of moso bamboo was set at 400 °C, 500 °C, 600 °C, and 700 °C, separately (Fig. 4), and the main compounds detected by coupled GC/MS of all samples are shown in Table 4. Relative peak areas were calculated for pyrolysis products with normalization of the summed areas of all the listed compounds. In Table 4, the main products from moso bamboo pyrolysis are identified as: ketones, aldehydes, esters, ethers, alcohols, furans, phenols, aromatic compounds, *etc*. Also, variances of the peak area and peak area % of these seven kinds of compounds with different pyrolysis temperatures are plotted in Fig. 5.

Table 4. Identification of the Pyrolysis Production Distribution by GC/MS

| No.	Compound Name	Formula	Group	Yield, Percent of Peak Area (%)			
				400 °C	500 °C	600 °C	700 °C
1	2-Butanone	C_4H_8O	ketones	—	4.28	4.76	5.57
2	Glycolaldehyde	$C_2H_4O_2$	aldehyde	—	4.70	7.61	8.56
3	2,3-Butanedione	$C_4H_6O_2$	ketones	—	2.29	2.11	2.69
4	3-Pentanone	$C_5H_{10}O$	ketones	—	2.82	3.83	3.68
5	Methyl acetate	$C_3H_6O_2$	esters	—	3.58	5.99	6.31
6	Ethyl propenyl ether	$C_5H_{10}O$	ethers	3.35	2.55	1.35	1.45
7	Methyl acetate	$C_3H_6O_2$	esters	3.54	4.14	4.55	4.67
8	Butanedial	$C_4H_6O_2$	aldehydes	—	5.35	4.40	4.57
9	Methyl 2-oxopropanoate	$C_4H_6O_3$	esters	—	2.25	2.42	2.53
10	Furfural	$C_5H_4O_2$	furans	3.20	3.71	2.96	2.96
11	6-Hydroxy- 2-Hexanone	$C_6H_{12}O_2$	ketones	1.30	3.25	2.26	1.83
12	Acetol acetate	$C_5H_8O_3$	ketones	—	0.94	0.85	0.87
13	2(5H)-Furanone	$C_4H_4O_2$	furans	—	2.32	1.66	1.75
14	Cyclohexanone	$C_6H_{10}O$	furans	1.77	3.87	3.50	3.50
15	2-Methoxy-4-propenylphenol	$C_8H_8O_3$	phenols	0.82	0.46	0.45	0.54
16	3-Hydroxy-4-methoxybenzyl alcohol	$C_{10}H_{12}O_2$	aromatic compounds	1.69	0.90	1.03	1.03
17	3-Methyl- 1,2-Cyclopentanedione	$C_6H_8O_2$	furans	—	1.96	1.86	1.79
18	Guaiacol	$C_7H_8O_2$	phenols	11.25	2.30	2.61	2.59
19	Cyclopropyl carbinol	C_4H_8O	alcohols	—	5.21	2.58	2.09
20	2,3-Dihydro-benzofuran	$C_8H_{10}O$	furans	26.61	8.53	10.25	8.87
21	3-Methoxy-1,2-Benzenediol	$C_8H_{10}O_2$	phenols	—	1.55	1.96	2.74
22	4-Ethyl-2-methoxyphenol	$C_7H_8O_3$	phenols	—	0.95	1.05	1.29
23	2-Methoxy-4-vinylphenol	$C_9H_{12}O_2$	phenols	7.52	3.88	3.70	3.76
24	2,6-Dimethoxyphenol	$C_9H_{10}O_2$	phenols	5.87	5.04	4.89	4.83
25	Eugenol	$C_8H_{10}O_3$	phenols	—	0.62	0.65	1.27
26	Vanillin	$C_7H_6O_2$	aromatic compounds	—	1.08	1.06	0.92
27	1,2,4-Trimethoxybenzene	$C_{10}H_{12}O_2$	aromatic compounds	—	1.85	2.04	1.90
28	2-Methoxy-4-(1-propenyl)-Phenol	$C_9H_{12}O_3$	phenols	3.72	2.46	2.36	2.47
29	5-Tert-Butylpyrogallol	$C_{10}H_{12}O_2$	phenols	—	1.10	0.86	0.72
30	3,5-Dimethoxyacetophenone	$C_{10}H_{14}O_3$	aromatic compounds	6.61	3.44	3.15	2.93
31	2,6-Dimethoxy-4-(2-propenyl)-phenol	$C_{10}H_{12}O_3$	phenols	—	1.25	1.17	1.15
32	3,5-Dimethoxy-4-hydroxybenzaldehyde	$C_8H_{16}O_2$	aromatic compounds	—	1.28	1.24	1.07
33	3-(4-Hydroxy-3-methoxyphenyl)-2-Propenoic acid	$C_{10}H_{12}O_3$	aromatic compounds	7.02	3.72	3.18	2.33
34	4-[(1E)-3-Hydroxy-1-propenyl]-2-methoxyphenol	$C_{11}H_{14}O_3$	phenols	6.50	2.84	2.54	2.30
35	3,5-Dimethoxy-4-hydroxyphenylacetic acid	$C_{11}H_{14}O_3$	aromatic compounds	3.42	1.47	1.13	1.11
36	3,5-Dimethoxy-4-hydroxycinnamaldehyde	$C_9H_{10}O_4$	aromatic compounds	3.68	0.98	1.29	0.94
37	2,5-Dimethoxy-benzenepropanoic acid	$C_{11}H_{14}O_3$	aromatic compounds	2.14	1.06	0.71	0.40
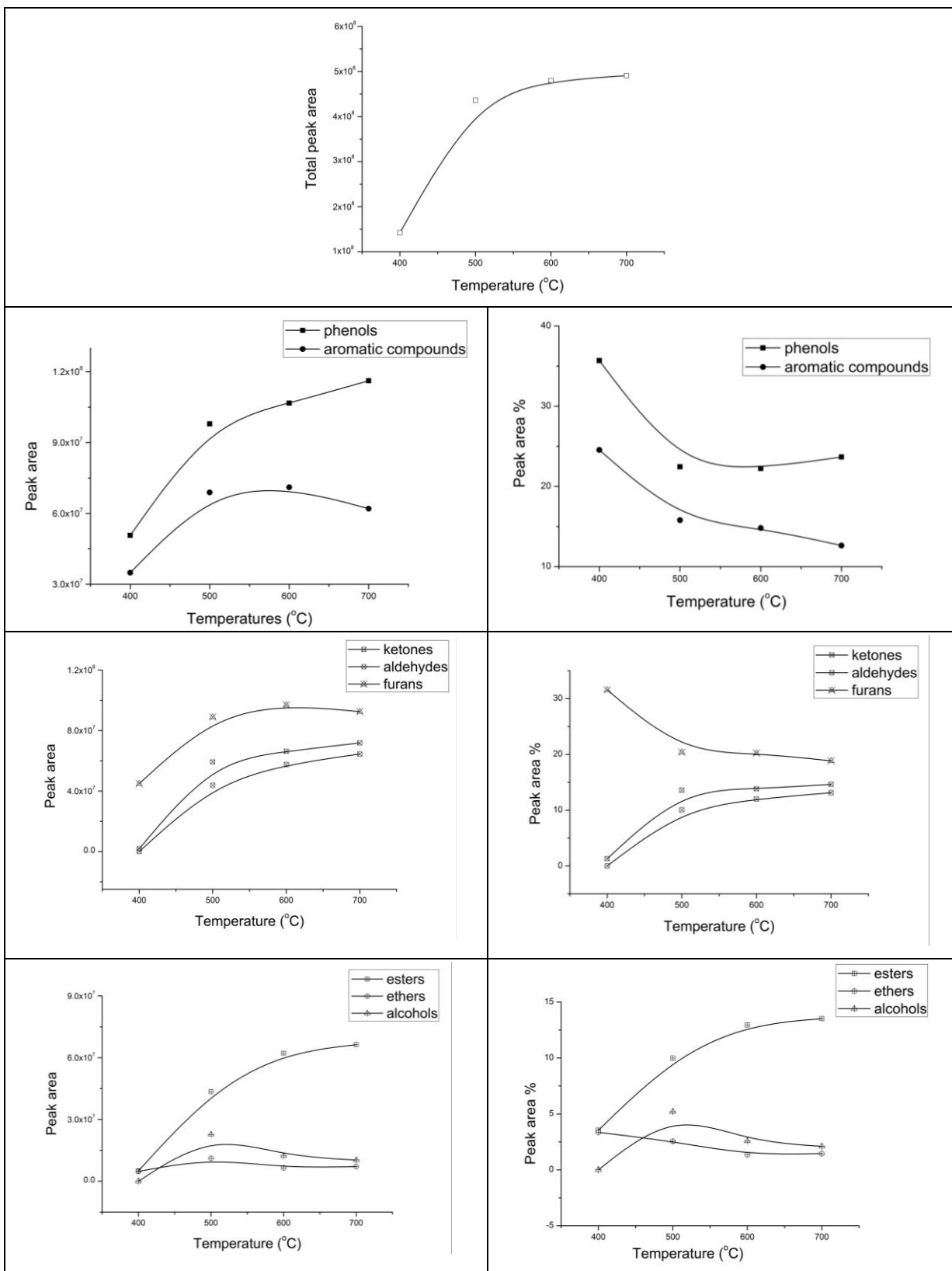
Fig. 5. Peak area and peak area % of the main compounds in pyrolysis vapors obtained from moso bamboo with different pyrolysis temperatures

bioresources.com

Due to the complexity of the pyrolytic vapors, it was hard to conduct the quantitative analysis of resulting compounds directly by Py-GC/MS. However, the chromatographic peak area of a compound is considered linear with its quantity, and the peak area % is linear with its content (Lu *et al.* 2012). Therefore, it is acceptable for the peak area value and peak area % to be compared to reveal the yields and relative contents of various typical compounds during one set of pyrolysis experiments.

As the pyrolysis temperature increased from 400 °C to 500 °C, the total peak area of GC/MS spectra rose sharply from 1.4×10^8 to 4.4×10^8. After this, the peak area increased slightly, which means that 500 °C was an inflection point for moso bamboo pyrolysis. Under 500 °C, moso bamboo decomposed softly and GC/MS detected few compounds. When temperature was increased from 500 °C to 700 °C, the increase in total peak areas was slow since the main components were almost degraded before arriving at the moderate temperature. Choi *et al.* (2012) also found that peak pyrolysis temperature for the maximum biocrude oil production was located at about 500 °C, and during this pyrolysis the temperature gasification reaction became dominant. The peak area of each compound had a similar pattern with large increases from 400 °C to 500 °C, but they began to be varied with different pathways after this peak temperature point. Generally, the relative content of phenols, ketones, and aldehydes increased while aromatic compounds and furans decreased by varying degrees, and esters and alcohols kept nearly constant.

It is generally known that aromatic compounds and phenols are mainly from the decomposition of lignin. Lignin typically degraded into guaiacol-type compounds at first and then guaiacols converted into phenols and catechols (Hoekstra *et al.* 2012). In the current study, there was an increase of phenols yields with a slight decrease of aromatic compound yields from 500 °C to 700 °C, which showed that aromatic compounds transferred into phenols by a further cracking reaction. Also, the methoxy group ($-OCH_3$) was thought to be an important source for the formation of the permanent gaseous species (Shen *et al.* 2010). Aldehydes and ketones mainly originated from the pyrolysis of hemicellulose and cellulose. Furans were the intermediates during the pyrolysis of cellulose and hemicellulose. Under 600 °C, the yields of furans rose gradually as the pyrolysis temperature increased. After this, a slight decrease in the yield of furans showed up from 600 °C to 700 °C, while yields of ketones and aldehydes increased at the same time. It was reasonable to assume that secondary cracking of furans contributed to the higher yield of the ketones and aldehydes. The yield of esters increased from 400 °C to 600 °C, and then kept almost constant. As for ethers and alcohols, their yield changed little. Esters were also thought to be degradation products mainly from polysaccharides.

In this study, slight changes among yields of aromatic, phenols, furans, ketones, and aldehydes under the effect of pyrolysis temperature were observed. After decomposition reactions of biomass matrix, reactions of produced vapors, aerosols, and solid residue happened in both a homogeneous and heterogeneous way, which affected the bio-oil yield and composition (Hoekstra *et al.* 2012). The secondary reactions here were regarded mostly to happen in a heterogeneous way, as there was enough time and there was an enclosed environment for the sample in the pyroprobe. Meanwhile, the pyrolysis vapor was largely diluted to very low consistence by the carrier gas of GC-MS after leaving the pyroprobe, which is not beneficial to the reactive collisions between reactants.

bioresources.com

CONCLUSIONS

1. The pyrolysis of moso bamboo was generally an integrated result of the decomposition of its several derived components, which was discovered by examining the degradation process parameters and pyrolysis kinetics obtained by thermogravimetric analysis.

2. Pyrolysis vapors from moso bamboo and derived components were analyzed by coupling FTIR and compared on the highest intensity point of gas release. The main peaks of the IR spectrum were assigned to be CO_2, CO, CH_4, H_2O, acids, aldehydes, aromatics, ethers, and alcohols.

3. Pyrolysis temperature played an important role in the products distribution of moso bamboo by affecting the producing yield and secondary cracking of heavy compounds. The inflection point for the release of pyrolysis vapors from moso bamboo occurred at 500 °C. A slight trend of further cracking of aromatic compounds and furans into lighter products was observed with increasing pyrolysis temperature.

ACKNOWLEDGMENTS

REFERENCES CITED

Azeez, A. M., Meier, D., Odermatt, J., Willner, T. (2010). "Fast pyrolysis of African and European lignocellulosic biomasses using Py-GC/MS and fluidized bed reactor," *Energy & Fuels*, 24(3), 2078-2085.

Bassilakis, R., Carangelo, R. M., Wojtowicz, M. A. (2001). "TG-FTIR analysis of biomass pyrolysis," *Fuel*, 80(12), 1765-1786.

Bridgwater, A. V. (2012). "Review of fast pyrolysis of biomass and product upgrading," *Biomass and Bioenergy*, 38, 68-94.

Choi, H. S., Choi, Y. S., Park, H. C. (2012). "Fast pyrolysis characteristics of lignocellulosic biomass with varying reaction conditions," *Renewable Energy*, 42, 131-135.

Coats, A. W., Redfern, J. P. (1964). "Kinetic parameters from thermogravimetric data," *Nature*, 201(491), 68.

Czernik, S., Bridgwater, A. V. (2004). "Overview of applications of biomass fast pyrolysis oil," *Energy & Fuels*, 18(2), 590-598.

Guo, D. L., Wu, S. B., Liu, B., Yin, X. L., Yang, Q. (2012). "Catalytic effects of NaOH and Na_2CO_3 additives on alkali lignin pyrolysis and gasification," *Applied Energy*, 95, 22-30.

Guo, J., Lua, A. C. (2001). "Kinetic study on pyrolytic process of oil-palm solid waste using two-step consecutive reaction model," *Biomass & Bioenergy*, 20, 223-233.

Hajallgol, M. R., Howard, J. B., Longwell, J. P., Peters, W. A. (1982). "Product compositions and kinetics for rapid pyrolysis of cellulose," *Industrial & Engineering Chemistry Process Design and Development*, 21(3), 457-465.

Hoekstra, E., Westerhof, R. J. M., Brilman, W., Van Swaaij, W. P. M., Kersten, S. R. A., Hogendoorn, K. J. A., Windt, M. (2012). "Heterogeneous and homogeneous reactions of pyrolysis vapors from pine wood," *AIChE Journal*, 58(9), 2830-2842.

Jiang, G., Nowakowski, D. J., Bridgwater, A. V. (2010). "A systematic study of the kinetics of lignin pyrolysis," *Thermochimica Acta*, 498(1-2), 61-66.

Jiang, Z., Liu, Z., Fei, B., Cai, Z., Yu, Y., Liu, X. (2012). "The pyrolysis characteristics of moso bamboo," *Journal of Analytical and Applied Pyrolysis*, 94, 48-52.

Jung, S. H., Kang, B. S., Kim, J. S. (2008). "Production of bio-oil from rice straw and bamboo sawdust under various reaction conditions in a fast pyrolysis plant equipped with a fluidized bed and a char separation system," *Journal of Analytical and Applied Pyrolysis*, 82(2), 240-247.

Kim, S. S., Park, S. H., Jeon, J. K., Chang, D., Kim, S. C., Lee, K. H., Park, Y. K. (2011). "Catalytic pyrolysis of waste wood chip over mesoporous materials using Py-GC/MS," *Research on Chemical Intermediates*, 37(9), 1355-1361.

Lédé, J. (2012). "Cellulose pyrolysis kinetics: An historical review on the existence and role of intermediate active cellulose," *Journal of Analytical and Applied Pyrolysis*, 94, 17-32.

Laird, D. A., Brown, R. C., Amonette, J. E., Lehmann, J. (2009). "Review of the pyrolysis platform for coproducing bio-oil and biochar," *Biofuels, Bioproducts and Biorefining*, 3(5), 547-562.

Li, S., Lyons-Hart, J., Banyasz, J., Shafer, K. (2001). "Real-time evolved gas analysis by FTIR method: an experimental study of cellulose pyrolysis," *Fuel*, 80, 1809-1817.

Lin, Y. C., Cho, J., Tompsett, G. A., Westmoreland, P. R., Huber, G. W. (2009). "Kinetics and mechanism of cellulose pyrolysis," *The Journal of Physical Chemistry C*, 113(46), 20097-20107.

Liu, B., Li, Y. M., Wu, S. B., Li, Y. H., Deng, S. S., Xia, Z. L. (2013). "Pyrolysis characteristic of tobacco stem studied by Py-GC MS, TG-FTIR and TG-MS," *BioResources*, 8(1), 220-230.

Liu, Q., Wang, S., Zheng, Y., Luo, Z., Cen, K. (2008). "Mechanism study of wood lignin pyrolysis by using TG–FTIR analysis," *Journal of Analytical and Applied Pyrolysis*, 82 (1), 170-177.

Lu, Q., Li, W. Z., Zhu, X. F. 2009. "Overview of fuel properties of biomass fast pyrolysis oils," *Energy Conversion and Management*, 50(5), 1376-1383.

Lu, Q., Zhang, X. M., Zhang, Z. B., Zhang, Y., Zhu, X. F., Dong, C. Q. (2012). "Catalytic Fast Pyrolysis of Cellulose Mixed with Sulfated Titania to Produce Levoglucosenone: Analytical Py-GC/MS Study," *BioResources*, **7**(3), 2820-2834.

Mamleev, V., Bourbigot, S., Yvon, J. (2007). "Kinetic analysis of the thermal decomposition of cellulose: The main step of mass loss," *Journal of Analytical and Applied Pyrolysis*, 80(1), 151-165.

Mui, E. L., Cheung, W. H., Lee, V. K., McKay, G. (2010). "Compensation effect during the pyrolysis of tyres and bamboo," *Waste Management*, 30(5), 821-830.

Ohra-aho, T., Tenkanen, M., Tamminen, T. (2005). "Direct analysis of lignin and lignin-like components from softwood kraft pulp by Py-GC/MS techniques," *Journal of Analytical and Applied Pyrolysis*, 74(1-2), 123-128.

Patwardhan, P. R., Brown, R. C., Shanks, B. H. (2011). "Product distribution from the fast pyrolysis of hemicellulose," *ChemSusChem*, 4(5), 636-643.

Ronsse, F., Bai, X., Prins, W., Brown, R. C. (2012). "Secondary reactions of levoglucosan and char in the fast pyrolysis of cellulose," *Environmental Progress & Sustainable Energy*, 31(2), 256-260.

Shen, D. K., Gu, S., Luo, K. H., Wang, S. R., Fang, M. X. (2010). "The pyrolytic degradation of wood-derived lignin from pulping process," *Bioresource Technology*, 101(15), 6136-46.

Yang, H., Yan, R., Chen, H., Lee, D. H., Zheng, C. (2007). "Characteristics of hemicellulose, cellulose and lignin pyrolysis," *Fuel*, 86(12-13), 1781-1788.

Zhang, M., Resende, F. L. P., Moutsoglou, A., Raynie, D. E. (2012). "Pyrolysis of lignin extracted from prairie cordgrass, aspen, and Kraft lignin by Py-GC/MS and TGA/FTIR," *Journal of Analytical and Applied Pyrolysis*, 98, 65-71.